International Journal of Automotive and Mechanical Engineering (IJAME)
ISSN: 2229-8649 (Print); ISSN: 2180-1606 (Online); Volume 7, pp. 811-819, January-June 2013

DOI: http://dx.doi.org/10.15282/ijame.7.2012.1.0066

SOUND AND VIBRATION SIGNAL ANALYSIS USING IMPROVED SHORT-TIME FOURIER REPRESENTATION

June-Yule Lee

Department of Marine Engineering, National Kaohsiung Marine University
482, Jhongjhou 3rd Road, Cijin District, Kaohsiung 80543, Taiwan
E-mail: juneyule@ms10.hinet.net

ABSTRACT

Time-frequency imaging provides a straightforward means to understanding machinery conditions. The methods of short-time Fourier transform (STFT), Wigner-Ville distribution (WVD) and smooth-windowed Wigner-Ville distribution (SWWVD) are applied to the condition monitoring of rotating machines. The sound and vibration signals of a rotating fan are tested, and time-frequency images are illustrated in terms of STFT, WVD and SWWVD. The results show that the resolution of STFT is low, and the resolution of WVD is high but with interference. To overcome the interference in the WVD image, a variable smooth-windowed weighting function is applied. The smoothing window function resulted in interference attenuation but also in reducing the concentration. The SWWVD is a compromise between STFT and WVD. The SWWVD exhibits better resolution than STFT and has less interference than WVD.

***Keywords*:** Time-frequency analysis; smooth window weighting; sound and vibration; condition monitoring.

INTRODUCTION

The sound and vibration signals of rotating systems have become more and more complex, as wind excitation, run up or shut down, rotor cracking and chattering can lead to frequency modulation and amplitude modulation. For the condition monitoring of these problems, the most important and fundamental variables in signal processing are time and frequency. The fundamental ideal of time-frequency analysis is to understand and describe those conditions where the frequency content of a signal changes in time. The short-time Fourier transform (STFT) is the most widely used tool for the display of stationary and non-stationary signals in time-frequency analysis. For better resolution, the quadratic time-frequency signal representation of the Wigner-Ville distribution (WVD) is considered. Unfortunately the WVD presents cross-terms (interferences) in multicomponent signals. Thus the WVD is a general tradeoff between good time-frequency resolution and small interference terms. Signals analysis simultaneously considered in time and frequency domain is well reviewed (Cohen, 1989; Hlawatsch and Boudreaux-Bartels, 1992; Nuawi et al., 2011; Hammond and White, 1996; Sejdic et al., 2009). In recent years, time-frequency methods have been widely used in gearbox fault detection (Staszewski et al., 1997), the diagnosis and surveillance of diesel engines based on vibration and acoustics signals (Delvecchio et al., 2010), and the vibration monitoring of rotating machines (Lee et al., 2001; Al-Badour et al., 2011; Climente-Alarcon et al., 2011; Peng et al., 2012). In this paper, a parameter-controlled smooth-windowed WVD method (SWWVD) is presented. The SWWVD allows the smoothing of the time spread and the smoothing of the frequency spread. In practical application, the sound and

vibration signals of a rotating fan are considered, and time-frequency images are illustrated in terms of STFT, WVD and SWWVD.

SHORT-TIME FOURIER TRANSFORM

The basic ideal of the short-time Fourier transform is that if one wants to know what frequencies exist at a particular time, then take a small part of the signal around that time and analyse it, neglecting the rest of signal. Since the time interval is short compared to the whole signal, this process is called a short-time Fourier transform. For a given signal x(t), the Fourier transform is

$$\mathrm{FT}(\mathrm{x(t)}) = \int_{-\infty}^{\infty} \mathrm{x(t)} \mathrm{e}^{-\mathrm{j}2\pi \mathrm{ft}} dt, \tag{1}$$

where f is frequency in Hz. Now we multiply the signal $\mathrm{x}(\tau)$ by a window function $\mathrm{w}(\tau - \mathrm{t})$ to obtain a weighted signal. Considering this signal as a function of τ and taking the Fourier transform, the STFT is

$$\mathrm{STFT}_x(t, f) = \int_{-\infty}^{\infty} x(\tau) w^*(\tau - t) e^{-j2\pi f\tau} d\tau, \tag{2}$$

where * is a complex conjugate. In Eq. (2), the smoothing window is applied by a parameter controlled function (Lee, 2010),

$$w(x:\alpha) = \begin{cases} \dfrac{\alpha}{2\beta\Gamma(1/\alpha)} \exp\left(-\left(\dfrac{-x}{\beta} \right)^{\alpha} \right) & \text{for } x < 0 \\ \dfrac{\alpha}{2\beta\Gamma(1/\alpha)} \exp\left(-\left(\dfrac{x}{\beta} \right)^{\alpha} \right) & \text{for } x > 0 \end{cases}, \tag{3}$$

where $\alpha > 0$, Γ is a gamma function and $\beta = \left(\Gamma(1/\alpha)/\Gamma(3/\alpha)\right)^{1/2}$. The parameter α controls the symmetric window shapes on the left side (x<0) and right side (x>0) in Eq. (3). The window shape of $\alpha = 1$ represents the Laplace distribution and $\alpha = 2$ represents the Normal distribution. When α tends to zero the function tends to an impulse distribution, and when α tends to infinity the function tends to a uniform distribution. Figure 1(a) shows the window shapes of $\alpha = 0.5$, 1, 2 and 10, and the corresponding spectrum plots are presented in Figure 1(b). For example, considering a multicomponent signal consisting of the sum of two chirp waveforms

$$s(t) = \sin(2\pi[f_1 t + 4t^2]) + \sin(2\pi[f_2 t - 4t^2]), \tag{4}$$

where $f_1 = 5$ Hz and $f_2 = 45$ Hz. Figure 2(a) shows the time series of Eq. (4) at a sampling rate 1 kHz. The signals include two non-stationary chirp waveforms. As time advances, the first chirp signals start at 5 Hz with increasing frequency, and the second chirp signals start at 45 Hz with decreasing frequency. The spectrum is shown in Figure 2(b), where information on the signal's frequency change over time is not provided. Using the STFT method and Figure 2 data, the time-frequency contour plot is shown in

Figure 3. The STTF image shows the complete information in the time and frequency domains. Two directions of moving frequency are illustrated, where the first and the second chirp signals cross at 2.5 seconds. The colour bar indicates the amplitude of the spectrum in intensity.

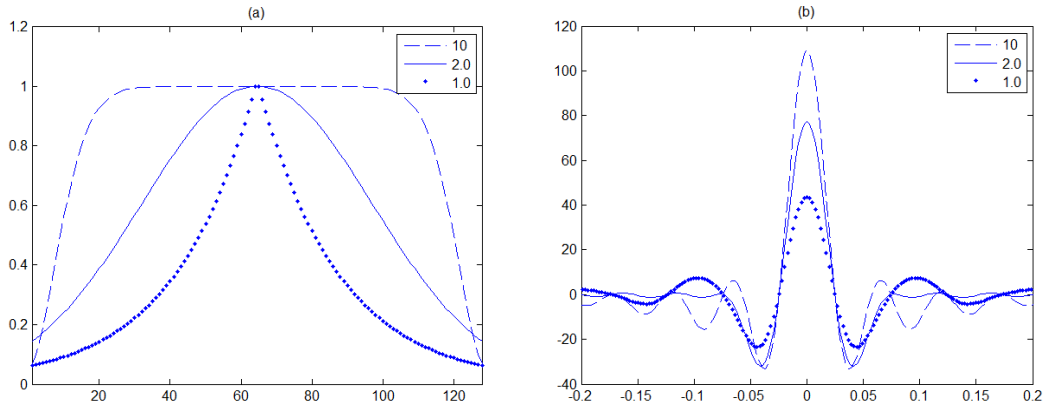

Figure 1. Smoothed window (N=128) for parameters α=1.0, 2.0 and 10; (a) time series, (b) spectrum.

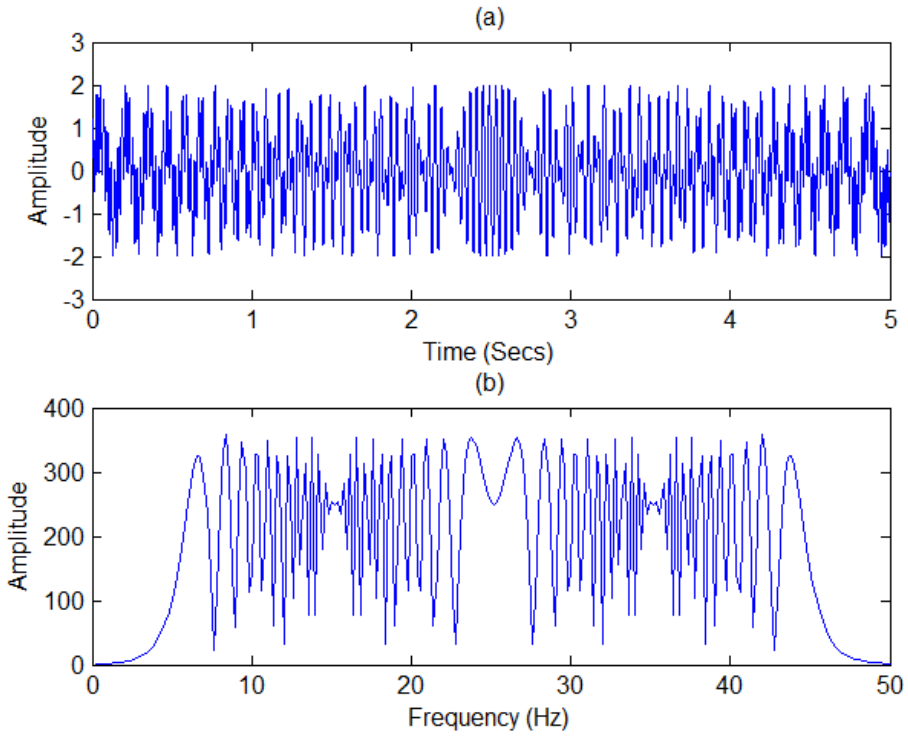

Figure 2. Simulation signals of the sum of two chirp waves: (a) time series, (b) spectrum.

WIGNER-VILLE DISTRIBUTION

The STFT suffers time-frequency resolution limitations: a good time resolution requires a short window weighting function and a good frequency resolution requires a long

window weight function. Thus a fundamental resolution tradeoff exists: it is impossible to simultaneously achieve both good time and frequency resolution. To improve the time-frequency resolution, a quadratic time-frequency representation of the Winger-Ville distribution is considered (Hlawatsch and Boudreaux-Bartels, 1992). For a signal x(t), the WVD is defined as

$$\mathrm{WVD}_x(t, f) = \int_{-\infty}^{\infty} x(t - \frac{\tau}{2}) x^*(t + \frac{\tau}{2}) e^{-j2\pi f\tau} d\tau. \tag{5}$$

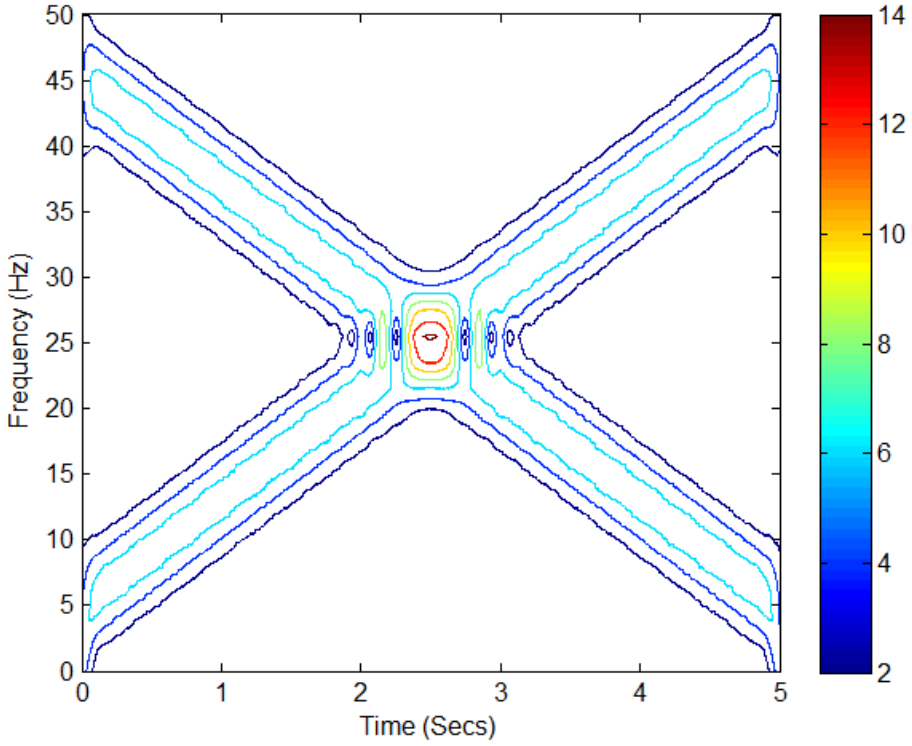

Figure 3. Time-frequency contour plot using STFT ($\alpha = 2$) method and Figure 2 data.

The STFT in Eq. (2) is a linear time-frequency representation to satisfy the superposition principle that if x(t) is a linear combination of some signal components, then the STFT of x(t) is the same linear combination. However, the quadratic representation of WVD in Eq. (5) is violated in terms of its linearity structure. Considering multicomponent signals $x(t) = x_1(t) + x_2(t)$, then WVD is given by

$$\mathrm{WVD}_x(t, f) = WVD_{x1x1}(t, f) + WVD_{x2x2}(t, f) + WVD_{x1x2}(t, f) + WVD_{x2x1}(t, f), \tag{6}$$

where

$$\mathrm{WVD}_{x1x2}(t, f) = \int_{-\infty}^{\infty} x_1(t - \frac{\tau}{2}) x_2^*(t + \frac{\tau}{2}) e^{-j2\pi f\tau} d\tau, \tag{7}$$

$$\mathrm{WVD}_{x2x1}(t, f) = \int_{-\infty}^{\infty} x_2(t - \frac{\tau}{2}) x_1^*(t + \frac{\tau}{2}) e^{-j2\pi f\tau} d\tau. \tag{8}$$

The WVD_{x1x1}, WVD_{x2x2} are auto-terms, and WVD_{x1x2}, WVD_{x2x1} are cross-terms which satisfy

$$WVD_{x1x2}(t, f) = WVD^{*}_{x2x1}(t, f). \tag{9}$$

Thus cross-terms $WVD_{x1x2}(t, f) + WVD_{x2x1}(t, f)$ is a real and Eq. (6) is written as

$$\mathrm{WVD}_{x}(t, f) = WVD_{x1x1}(t, f) + WVD_{x2x2}(t, f) + 2\,\mathrm{Re}[WVD_{x1x2}(t, f)]. \tag{10}$$

Equation (10) indicates that the WVD of the sum of the two signals is not only the sum of two auto-terms, but also includes the cross-terms. These cross-terms cause interference in the distribution over both time and frequency. For example, using the WVD method and Figure 2 data, the time-frequency contour plot is shown in Figure 4. As expected, the WVD image shows a high concentration when compared to the STFT in Figure 3. But the cross-terms (interference) occurs midway between the two chirp signals.

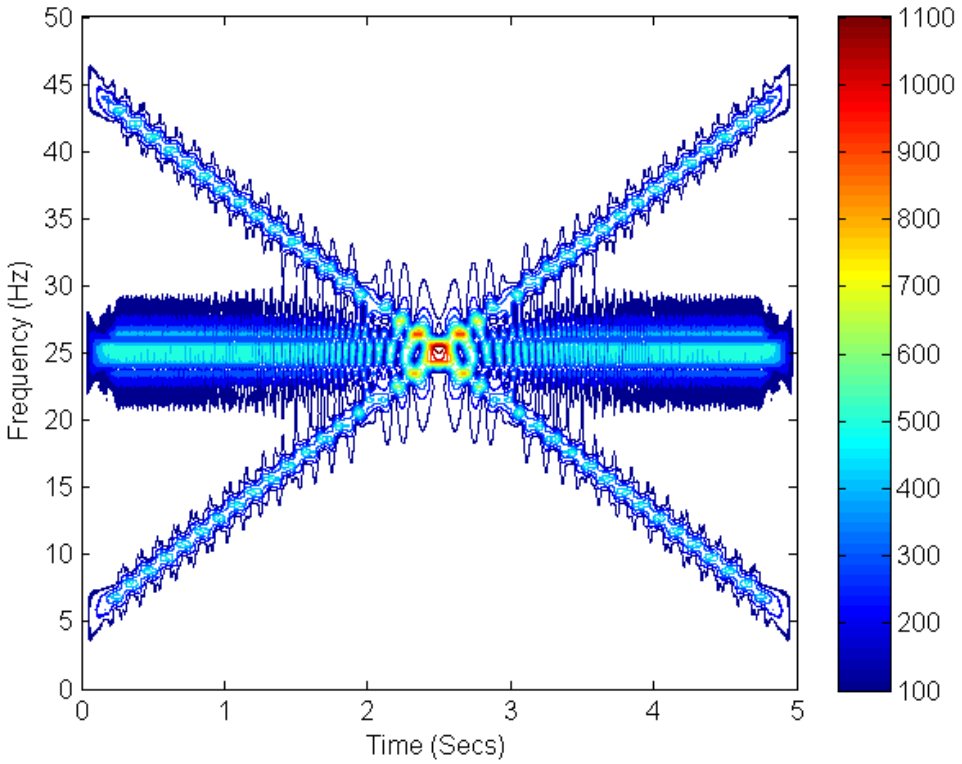

Figure 4. Time-frequency contour plot using WVD method and Figure 2 data.

SMOOTH-WINDOWED WIGNER-VILLE DISTRIBUTION

In practical applications, the interference terms of WVD are often a problem for condition monitoring. In order to suppress the cross-terms, a window weighted method is applied. Two smoothed windows are processed for WVD in both the time and frequency direction.

This is a smooth-windowed Wigner-Ville distribution and is defined as

$$\text{SWWVD}_x(t, f) = \int_{-\infty}^{\infty} h(\tau) \int_{-\infty}^{\infty} g(s-t) x(s-\frac{\tau}{2}) x^*(s+\frac{\tau}{2}) ds e^{-j2\pi f\tau} d\tau \qquad (11)$$

where h(t) and g(t) are smoothing windows for time and frequency, respectively. In the following investigation, the window function in Eq. (3) is applied for h(t) and g(t).

The smoothing window process resulted in interference attenuation, but also in reducing the time-frequency concentration. Thus the SWWVD is a compromise of STFT and WVD. For example, using the SWWVD method and Figure 2 data, the time-frequency contour plot is shown in Figure 5. As expected, the interference terms in Figure 4 are suppressed in both the time and frequency directions. The colour bar of Figure 5 show that the intensity is reduced when compared to Figure 4. However, the resolution is far better than in Figure 3. Thus the SWWVD shows a compromise result between STFT and WVD. The SWWVD has better resolution than STFT and has less interference than WVD.

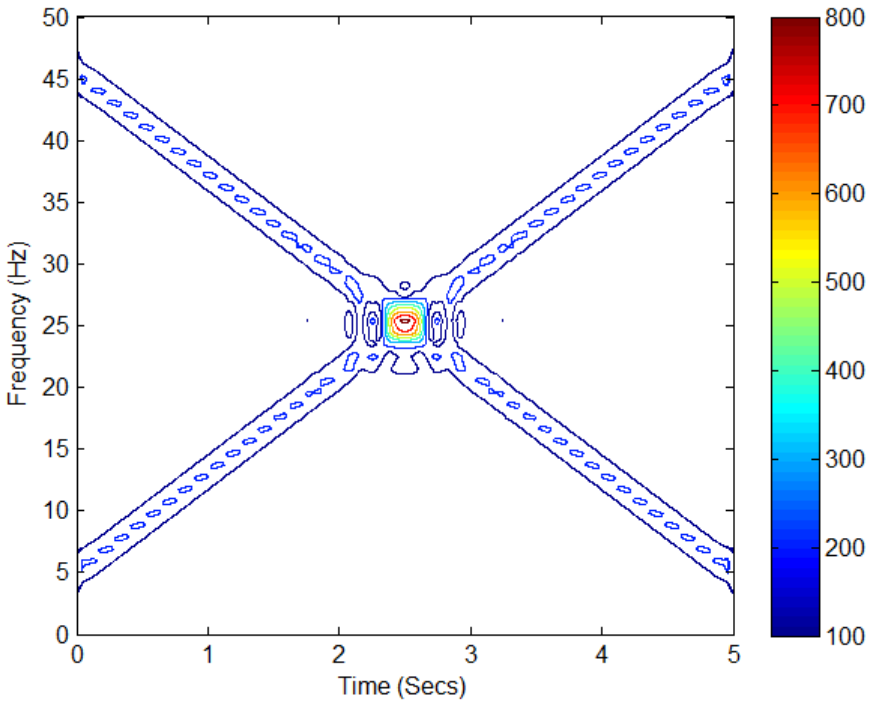

Figure 5. Time-frequency contour plot using SWWVD ($\alpha = 10$) method and Figure 2 data.

SOUND AND VIBRATION SINGALS ANALYSIS

For application in condition monitoring, the above methods are applied to real rotating fan signals. Figure 6 shows the measured vibration (acceleration) and sound pressure signals at a sampling rate of 25 kHz, and the corresponding spectra are shown in Figure 7. The vibration signal shows two resonance peaks located at 150 and 700 Hz; and the main peak of the acoustic noise is located at 180 Hz. Using the vibration signals in Figure 6(a)

and the acoustic noise in Figure 6(b), the time-frequency contour plots of the STFT, WVD and SWWVD methods are illustrated in Figures 8, 9 and 10, respectively. As expected, the STFT image shows the frequency content in time, but the time-frequency resolution is poor. The WVD image shows a high resolution but with interference in the time and frequency domains. Thus for multicomponent signals analysis, the STFT and WVD methods might mislead the system conditions due to the low resolution or interference. However, the SWWVD image indicates that the interference is significantly reduced and has better resolution than the STFT method.

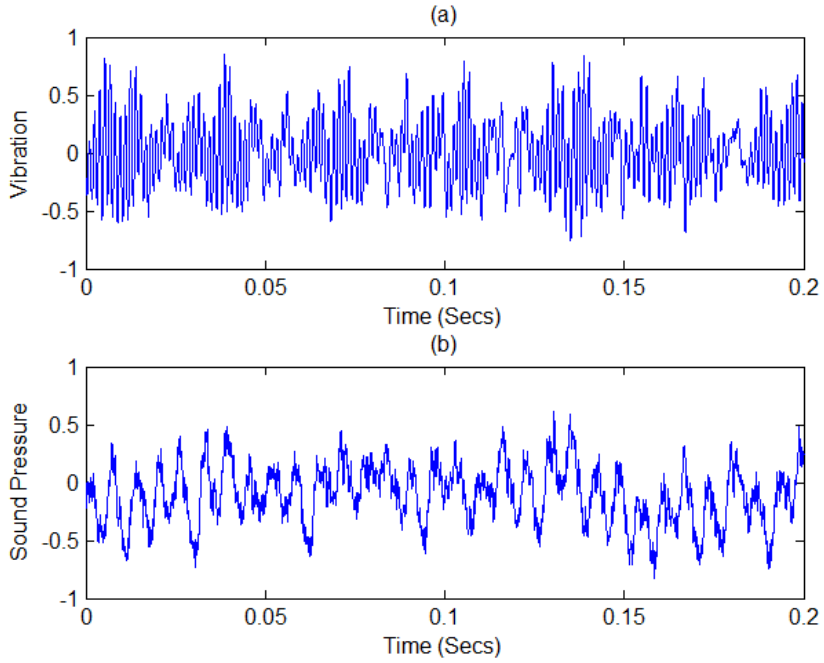

Figure 6. Time series of rotating fan signals: (a) vibration, (b) sound pressure.

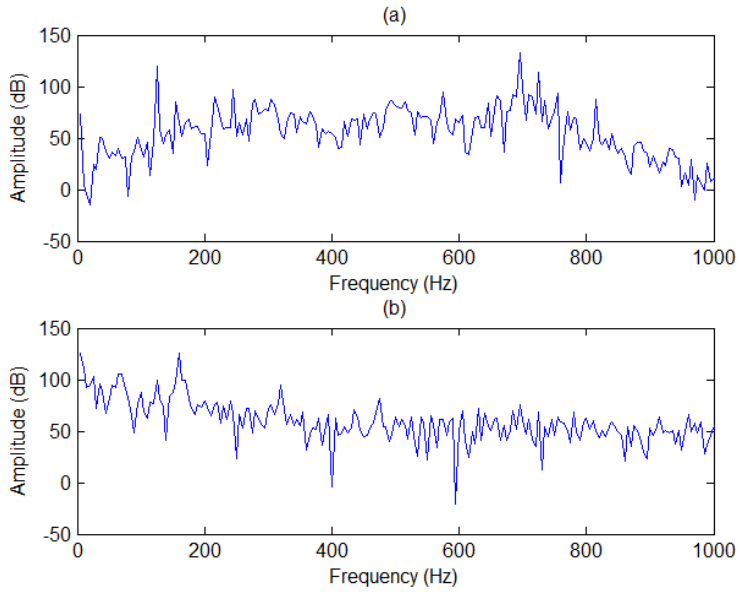

Figure 7. Spectrum of rotating fan signals: (a) vibration, (b) sound pressure.

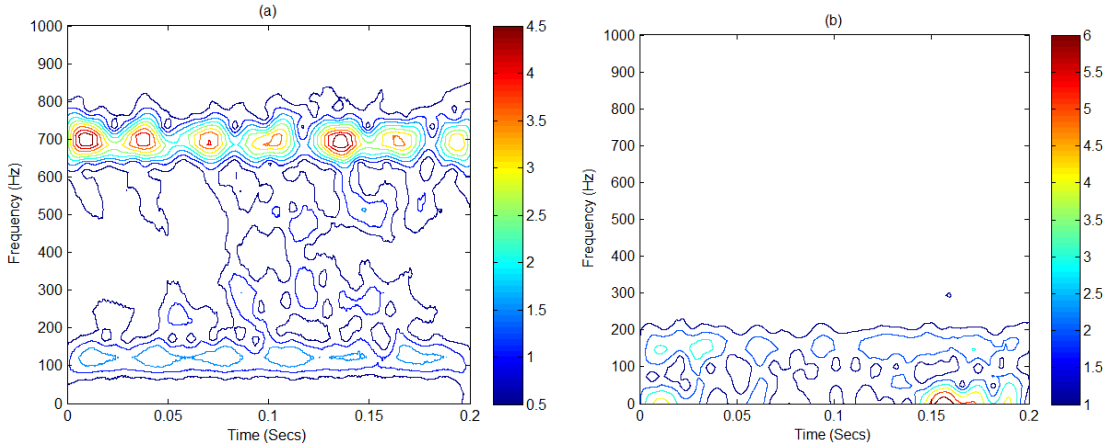

Figure 8. Time-frequency contour plots using STFT (α =2) method and Figure 6 data: (a) vibration, (b) sound pressure.

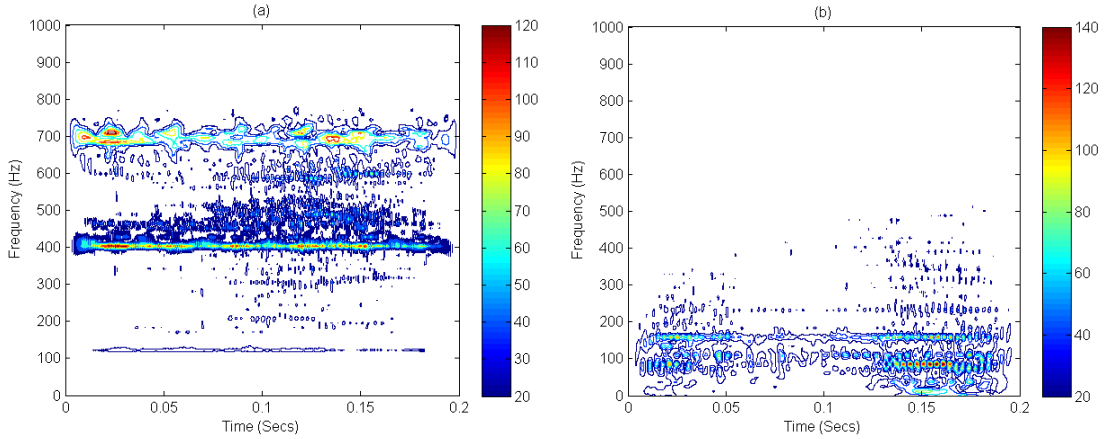

Figure 9. Time-frequency contour plots using WVD method and Figure 6 data: (a) vibration, (b) sound pressure.

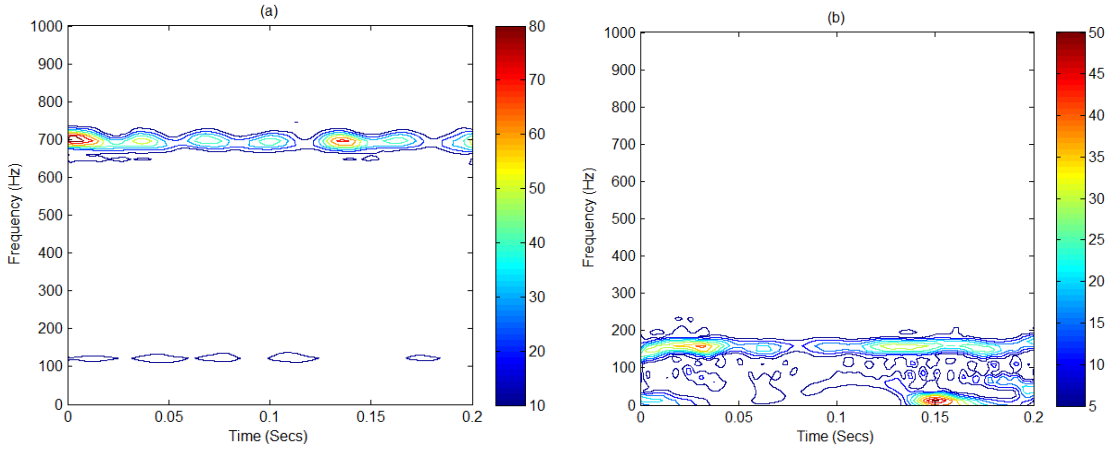

Figure 10. Time-frequency contour plots using SWWVD (α =10) method and Figure 6 data: (a) vibration, (b) sound pressure.

CONCLUSION

The time-frequency representations of the STFT, WVD and SWWVD methods are presented and applied to the condition monitoring of a rotating system. The results demonstrate that the time-frequency image is a straightforward means to understanding machinery conditions. To improve the resolution of the SFFT and to overcome the interference of the WVD, parameter control of the smooth-windowed SWWVD method is demonstrated. The results show that SWWVD is a compromise version between STFT and WVD. The SWWVD has better resolution than STFT and less interference than WVD.

REFERENCES

Al-Badour, F., Sunar, M. and Cheded, L. 2011. Vibration analysis of rotating machinery using time-frequency analysis and wavelet techniques. Mechanical Systems and Signal Processing, 25: 2083-2101.

Climente-Alarcon, V., Antonino-Daviu, J., Riera-Guasp, M., Pons-Llinares, J., Roger-Folch, J., Jover-Rodriguez, J. and Arkkio, A. 2011. Transient tracking of low and high-order eccentricity-related components in induction motors via TFD tools. Mechanical Systems and Signal Processing, 25: 667-679.

Cohen, L. 1989. Time-frequency distributions: A review. Proceedings of the IEEE, 77(7): 941-981.

Delvecchio, S., D'Elia, G., Mucchi, E. and Dalpiaz, G. 2010. Advanced signal processing tools for the vibratory surveillance of assembly faults in diesel engine cold tests. ASME Journal of Vibration and Acoustics, 132(021008): 1-10.

Hammond, J.K. and White, P.R. 1996. The analysis of non-stationary signals using time-frequency methods. Journal of Sound and Vibration, 190(3): 419-447.

Hlawatsch, F. and Boudreaux-Bartels, G.F. 1992. Linear and Quadratic Time-frequency Signal Representations. IEEE Signal Processing Magazine, 9: 21-67.

Lee, J.Y. 2010. Parameter estimation of the extended generalized gaussian family distributions using maximum likelihood scheme. Information Technology Journal, 9(1): 61-66.

Lee, S.U., Robb, D. and Besant, C. 2001. The directional Choi-williams distribution for the analysis of rotor-vibration signals. Mechanical Systems and Signal Processing, 15(4): 789-811.

Nuawi, M.Z., Ismail, A.R., Nor, M.J.M. and Rahman, M.M. 2011. Comparative study of whole-body vibration exposure between train and car passengers: a case study in Malaysia. International Journal of Automotive and Mechanical Engineering, 4: 490-503.

Peng, Z.K., Zhang, W.M., Lang, Z.Q., Meng, G. and Chu, F.L. 2012. Time-frequency data fusion technique with application to vibration signal analysis. Mechanical Systems and Signal Processing, 29: 164-173.

Sejdic, E., Djurovic, I. and Jiang, J. 2009. Time-frequency feature representation using energy concentration: an overview of recent advances. Digital Signal Processing, 19: 153-183.

Staszewski, W., Worden, K. and Tomlinson, G.R. 1997. Time-frequency analysis in gearbox fault detection using the wigner-ville distribution and pattern recognition. Mechanical Systems and Signal Processing, 11(5): 673-692.